

Study of the Ni(n,p)Co Reaction*†

L. D. SINGLETARY

Lockheed Missiles and Space Company, Palo Alto, California

E. N. STRAIT

Northwestern University, Evanston, Illinois

AND

S. H. AHN

Yonsei University, Seoul, Korea

(Received 15 May 1963)

The total cross section and energy spectrum for the (n,p) reaction on nickel has been measured for 15-MeV neutrons using a modified broad-range magnetic spectrograph and nuclear emulsions. Proton spectra were measured at scattering angles of 0° and 138° . A nuclear temperature of 1 MeV was determined from the 138° spectrum. If isotropy of the compound nucleus reaction products is assumed, the cross section for the compound nucleus part of the (n,p) reaction can be estimated as 650 ± 150 mb. The additional contribution from direct interaction is estimated as 160 ± 80 mb.

INTRODUCTION

THIS experiment is an attempt to add some significant information to the body of data on nuclear reactions produced by high-energy particles (10 to 20 MeV). The most generally studied reactions in this energy region are inelastic scattering of neutrons and protons. Neutron-induced reactions in which charged secondary particles are emitted have also been studied recently. In either case, one might expect the statistical model continuum theory to account for the total cross sections, energy distributions and finally angular distributions. However, this is found not to be entirely correct. It was suspected that some of the discrepancies observed might be explained by carefully identifying the types of charged particles as well as measuring their energies. Many of the previous experiments were performed with no means of adequately identifying the charged particles.

The present work was undertaken to provide identification of the outgoing charged particles in reactions produced by 15-MeV neutrons on nickel and to measure the yields and angular distribution of these particles. Several investigators have measured the cross sections and nuclear temperatures associated with (n,p) reactions in nickel.¹⁻⁸ Results from these experiments are discussed and compared with the present data in the section on discussion of results.

DISCUSSION OF EXPERIMENT

In the experiment reported here, measurements were made which differentiate among protons, deuterons, and alpha particles. Total and differential cross sections were determined for the proton component. A broad-range charged particle spectrograph was adapted for this purpose. Natural nickel was bombarded by 15-MeV neutrons and the charged particles were detected on nuclear emulsions at the exit pole face of the spectrograph. A schematic view of the experimental arrangement is shown in Fig. 1.

Exposures were made at three different momentum settings which covered the proton energy range from 2 to 16 MeV. The measurements were repeated at four different angles of observation relative to the neutron beam: 0 , 45 , 90 , and 138 deg.

The neutrons in this experiment were produced by the $H^3(d,n)He^4$ reaction with a tritium gas target and deuterons accelerated by an electrostatic accelerator. The very high Q of the reaction, 17.578 MeV, makes possible the production of high-energy neutrons with relatively low incident deuteron energy, and by selecting the laboratory angle it can provide neutrons of from 12 to 20 MeV by using deuterons of energy up to 3 MeV. With gas targets the limitation on the neutron flux obtainable is usually due to heating and thus weakening of the foil window by the deuteron beam. The cooling system of the present gas target was a modification of the system of Nobles.⁹ A cooling channel was formed between two molybdenum foils of 0.0004 in. thickness placed upstream of the tritium cell proper. The tritium target was designed to completely stop 600-keV deuterons.

The beam of deuterons approaching the tritium was collimated by a series of tantalum apertures ranging from $\frac{5}{16}$ in. to $\frac{1}{4}$ in. in size. The first one, lying nearest the beam entrance channel, had two small holes lying

* Supported in part by the Lockheed Missiles and Space Company Independent Research Fund.

† This work was based on a thesis submitted by L. D. S. to Northwestern University in partial fulfillment of the requirements for the degree of Doctor of Philosophy.

¹ D. L. Allan, Proc. Phys. Soc. (London) **70**, 195 (1957).

² F. V. March and W. T. Morton, Phil. Mag., **3**, 577 (1958).

³ L. Colli, U. Facchini, I. Iori, M. G. Marazzan, and A. M. Sona, Nuovo Cimento **13**, 730 (1959).

⁴ I. Kumabe and R. W. Fink, Nucl. Phys. **15**, 316 (1960).

⁵ R. S. Storey, W. Jack, and A. Ward, Proc. Phys. Soc. (London) **75**, 526 (1960); W. Jack and A. Ward, *ibid.* **75**, 833 (1960).

⁶ R. N. Glover and K. H. Purser, Nucl. Phys. **24**, 431 (1961).

⁷ D. L. Allan, Nucl. Phys. **24**, 274 (1961).

⁸ F. L. Hassler and R. A. Peck, Jr., Phys. Rev. **125**, 1011 (1962).

⁹ R. Nobles, Rev. Sci. Instr. **28**, 962 (1957).

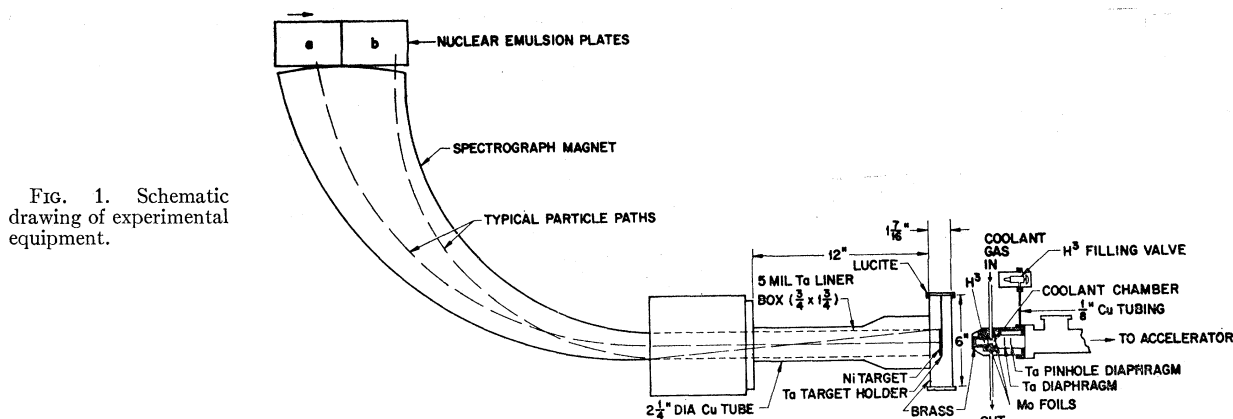


FIG. 1. Schematic drawing of experimental equipment.

on a diameter at equal distances from the beam centerline. To observe the beam, it could be swept past these holes. The transmitted portion, picked up on the second tantalum aperture, generated an electrical signal which controlled the intensity of an oscilloscope beam swept in synchronism with the deuteron beam.

To prevent rupturing the foil, the condition of focus and the position of the beam were monitored by the observation of the beam-scanner oscilloscope. Fine adjustments of the focus and position could be easily made using a set of strong focusing magnetic quadrupoles and steering magnets mounted on the beam line. In case the focus became too sharp for any reason, a small radius of sweep was maintained so the beam would not dwell in one spot and possibly burn a hole in the foil.

Natural nickel was chosen as a suitable target. It has a magic number of protons, $Z=28$. Both the principal isotopes, Ni^{58} and Ni^{60} , are neutron deficient, and contain 30 and 32 neutrons, respectively. They have Q values which are very close to zero for the (n, p) reaction, and large (n, p) cross sections. Nickel is easily available and is not reactive or easily contaminated with impurities.

Nickel targets consisted of 1-mil or of $\frac{1}{2}$ -mil nickel foil made by the Chromium Corporation of America. Targets 1 in. \times 2 in. were fastened to 20-mil tantalum target holders. The solid angle between the source and target was 0.36 sr with an average angle of 15° . The target backing and the inside of the tubing leading from the target chamber to the spectrograph were lined with tantalum, chosen for its low (n, p) cross section.

The $\frac{1}{2}$ -mil nickel target was used for the two lower momentum settings; the 1-mil target for the higher setting corresponding to a proton energy range of 8 to 16 MeV. The thicker target was used in the latter case because the cross sections for (n, p) reactions decrease rapidly at higher energies of the emitted particle. Also, the energy loss in the target becomes less significant since dE/dx drops as the energy of the particle emitted increases.

A broad-range spectrograph with a 20-in. radius

similar to the one developed by Browne and Buechner¹⁰ was used in the present experiment. The entrance slit to the spectrograph was $\frac{1}{2}$ in. \times $\frac{3}{8}$ in. The magnetic field was measured and controlled by a floating limp wire and associated circuitry. The spectrograph was calibrated to $\frac{1}{2}\%$ in energy by passing successively beams of energy 2.56 and 4.6 MeV and a diatomic hydrogen beam of energy 4.6 MeV directly into the spectrograph and focusing them on a quartz viewer at the exit pole face.

Two glass-backed nuclear emulsions 3 in. \times $4\frac{1}{2}$ in. were mounted directly at the exit pole face of the spectrograph rather than at its focal plane. Their surfaces made an angle of 11° with the particle directions. This plate location resulted in a reduction by a factor of four of the emulsion area to be scanned, but a sacrifice of some of the energy resolution of the spectrograph since each position on the plate is accessible to a range of trajectory radii.

As a result, particle energies were best determined by track length measurements and the spectrograph served primarily to distinguish between proton, deuteron and alpha particle groups. A graphical analysis was performed to determine values of possible particle radius for each position, x , along the plate (see Fig. 1). From the energy calibration mentioned above, curves of particle radius versus energy are obtained for each magnetic field setting. Combining these two sets of data along with range-energy relations from Allred and Armstrong¹¹ results in plots of allowed range versus plate position for protons, deuterons and alphas as shown in Fig. 2 for one magnetic field value.

Two large blocks of iron, 5 in. \times $2\frac{1}{2}$ in. \times 18 in., shielded the camera box from the direct neutron source. They were suspended from the top of the spectrograph at 26° from the vertical. The iron shielding reduced the number of direct 15-MeV neutrons reaching the emulsions by approximately a factor of 3×10^3 . A 4-in.

¹⁰ W. W. Buechner and C. P. Browne, Rev. Sci. Instr. **27**, 899 (1956).

¹¹ J. C. Allred and A. H. Armstrong, Laboratory Handbook of Nuclear Microscopy, LA-1510, 1950 (unpublished).

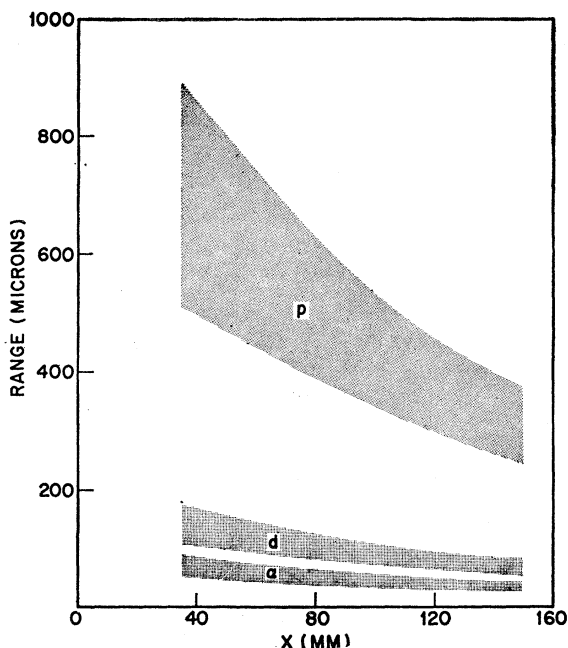


FIG. 2. Separation of particles by the spectrograph.

thickness of paraffin was stacked all around the camera box to reduce the number of room scattered neutrons reaching the plates. This shielding reduced the background by a factor of two. With the above shielding, signal-to-background ratios were about 20:1 for protons above 8 MeV and decreased to about 5:1 for lower energy protons.

The emulsions were Ilford G-special, 200- and 100- μ thick. The development procedure was a modification of a temperature development technique of the Livermore Nuclear Film Group,¹² in that there was no agitation of solutions throughout.

Two successive exposures, one "signal" and one "background," were made at each of three different momentum settings which covered the proton energy range from 2 to 16 MeV. These exposures were repeated at four different angles of observation relative to the neutron beam; 0, 45, 90, and 138 deg. The signal exposure was identical to the background exposure except that in the former case a nickel foil was fastened to the 20-mil tantalum holder in the target position, while in the latter case there was only the 20-mil tantalum holder. In general, the background runs were only three fifths as long as the signal runs.

In order to establish the absolute neutron flux, the solid angle of the spectrograph was measured by means of additional exposures at the 0-deg angle using a 1-mil polyethylene target instead of the nickel. These exposures also served to extend the energy calibration to 14 MeV. The magnetic field settings were such as to direct the elastically scattered protons from the

hydrogen in the polyethylene to various positions at the spectrograph exit.

A current integrator provided information about the total deuteron flux incident on the tritium cell. The neutron intensity was monitored during the experiment by a plastic scintillator 1 in. in diameter by $1\frac{1}{2}$ -in. thick which was mounted 6 ft from the neutron source. In order to maintain constant neutron energy and maximum intensity, a yield curve across the 100-keV resonance of the $H^2(d,n)He^4$ reaction was made at least once each day. The deuteron energy was adjusted to provide the maximum neutron yield during the exposures. On no occasion did the required deuteron energy depart by more than 5% from the mean. Such departures showed no systematic trend which might be indicative of tritium loss or accumulation of carbon on the foils.

For each exposure, the integrated flux was determined by counting the activity in zirconium cylinders $\frac{1}{4}$ in. in diameter and $\frac{3}{8}$ -in. long which had been placed close to the neutron source. A coincidence counting system was set up to measure the annihilation gammas from positron decay of Zr^{89} produced during an experimental run.

EMULSION SCANNING AND DATA ANALYSIS

In examining tracks in the emulsions certain measurement criteria were imposed to help distinguish between tracks due to true events and spurious ones. Particles which originated in the target and were deflected through the spectrograph caused tracks which started at the emulsion surface and were collimated. Spurious tracks of proton recoils due to neutrons incident on the emulsion had very small probability of starting at the emulsion surface and had no preferred direction. By imposing selection criteria that require tracks to start at the surface and have proper orientation in the emulsion, it was possible to discriminate against background tracks.

Each of the four binocular research microscopes used to scan emulsions were equipped with a goniometer device to measure φ , the angle between the track direction and a fixed line in the plane of the emulsion. The eyepieces were equipped with a graduated scale to measure projected track length, R_p . The depth of dive of tracks in the emulsion, δ , could be measured to the nearest micron. The magnification used for measurement varied depending on the range of the tracks on a particular plate. In general, eyepieces of 10 \times and objectives of 12.5 \times to 40 \times were used. The limits on the angle φ were determined by measuring at various positions on the emulsion the distribution in φ of the knock-on proton tracks from the polyethylene target. The acceptance criteria on depth of dive, δ , is calculated from the spectrograph geometry and also is consistent with data from the polyethylene. The acceptable range of R_p is determined by the setting of the magnetic field of the spectrograph for a particular plate.

¹² J. B. Marion and J. L. Fowler, *Fast Neutron Physics* (Interscience Publishers, Inc., New York, 1960), Part 1, Chap. II D.

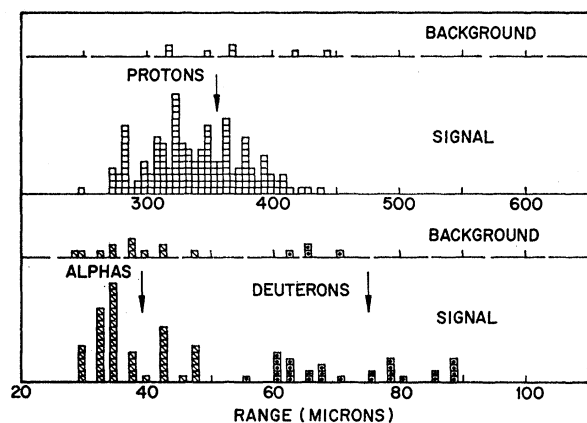


Fig. 3. Typical histogram of tracks measured for one of the data points.

Each nuclear emulsion glass plate had a contact printed millimeter grid glued to its back. Each square millimeter had its x and y coordinates printed on it. A special stage was made for each microscope which allowed freedom to position the plate. The emulsion was then generally scanned in swaths approximately 60 mm long parallel to the y axis and 1-mm wide. Stops were designed for the microscopes which defined the 1-mm width of scan.

Sixty-two plates were exposed, two during each of the 31 exposures. In the course of a year, scanning was done on 21 of the plates with roughly $\frac{2}{3}$ of the area scanned being on signal plates and the remainder on background. The total number of signal tracks measured was 971 and the number of background tracks was 177. These numbers do not include the polyethylene knock-on proton tracks measured for calibration purposes or those tracks measured to establish angle criteria.

Each measured track was identified and tabulated using a curve of the type shown in Fig. 2. Histograms as shown in Fig. 3 were made for each of the data points which were studied. A data point has an average energy spread of 1 MeV.

Weighting factors were applied to take account of the relative areas scanned and the relative neutron exposures. Background counts were subtracted from the signal count. Corrections for the energy loss of the emitted charged particles in the nickel foil or polyethylene have been made. The energy losses to be expected in the foil were determined principally with the aid of stopping power data given by Whaling.¹³ For proton energies above 10 MeV the tabulations of Aron *et al.*¹⁴ were used. The correction curve for nickel was determined from their data on copper. It was assumed that all particles observed originated in the

middle of the foil used. Other corrections were made to take account of departures from good geometry.

The differential cross section per MeV for each point was then determined using the relation

$$\sigma_N(\epsilon, \theta) = \frac{W_N N_p \sigma_p(\theta) (\Omega_c/\Omega_L)_p \Omega_{L,p}}{W_p N_N \Delta \epsilon (\Omega_c/\Omega_L)_N \Omega_{L,N}},$$

where W = number of tracks measured normalized for area and exposure, at a given x scanning point, N = number of atoms in target, $\Omega_c = (\Omega_c/\Omega_L)\Omega_L$ = solid angle in center-of-mass system, $(\Omega_c/\Omega_L)_N$ = solid-angle ratio for nickel, $(\Omega_c/\Omega_L)_p$ = solid-angle ratio for polyethylene = 3.79, $\Omega_{L,p} = \Omega_{L,N}$ = solid angle in laboratory system (same for both nickel and polyethylene scatterers), $\sigma_p(\theta)$ = polyethylene differential cross section in center-of-mass system = 650/4 π mb/sr, $\Delta \epsilon$ = energy width for the plate point in question, W_p = number of polyethylene tracks = 1154, and ϵ = energy of emitted particle.

Substituting the appropriate constants leads to

$$\sigma_N(\epsilon, \theta) = W_N \frac{5.3 \times 10^{20}}{N_N (\Omega_c/\Omega_L)_N}.$$

For the case of the general reaction, $x + a \rightarrow C^* \rightarrow Y^* + b$, the level density, ω_Y , associated with the residual nucleus Y from the statistical model can be written

$$\omega_Y(\epsilon) = K \sigma(\epsilon, \theta) / \epsilon \sigma_c(\epsilon),$$

where ϵ = excitation energy of the residual nucleus, $\sigma_c(\epsilon)$ = cross section for the formation of a compound system C^* by particle b interacting with the excited nucleus Y^* , K = constant of proportionality, and it has been assumed that $\sigma(\epsilon, \theta)$ is isotropic.

The conventional statistical theory plot was made of $\ln \omega_Y$ versus ϵ , with the nuclear temperature T being derived from the slope of this curve. The σ_c 's used are from the tables of Shapiro¹⁵ which are based on accurate values of the Coulomb wave functions and give σ_c for bombardment of ground state nuclei by protons, deuterons, and alphas of various energies.

DISCUSSION OF RESULTS

The energy distributions for the (n, p) reaction on nickel at 0° and 138° angles are presented in Figs. 4 and 5. The curves represent the contribution due to compound nucleus processes alone and are discussed below.

No levels were resolved among the several isotopes of nickel in the target. Referring to the nuclear level schemes of Way *et al.*,¹⁶ it is seen that these isotopes have level spacings of the order of 100 to 400 keV near the ground state. Naturally, the spacing decreases

¹³ W. Whaling, in *Handbuch der Physik*, edited by S. Flügge (Springer-Verlag, Berlin, 1958), Vol. 34, p. 193.

¹⁴ W. A. Aron, B. G. Hoffman, and F. C. Williams, AECU-663, UCRL-121, 1949 (unpublished).

¹⁵ M. M. Shapiro, *Phys. Rev.* **90**, 171 (1953).

¹⁶ *Nuclear Data Sheets*, compiled by K. Way *et al.* (Printing and Publishing Office, National Academy of Sciences-National Research Council, Washington 25, D. C.).

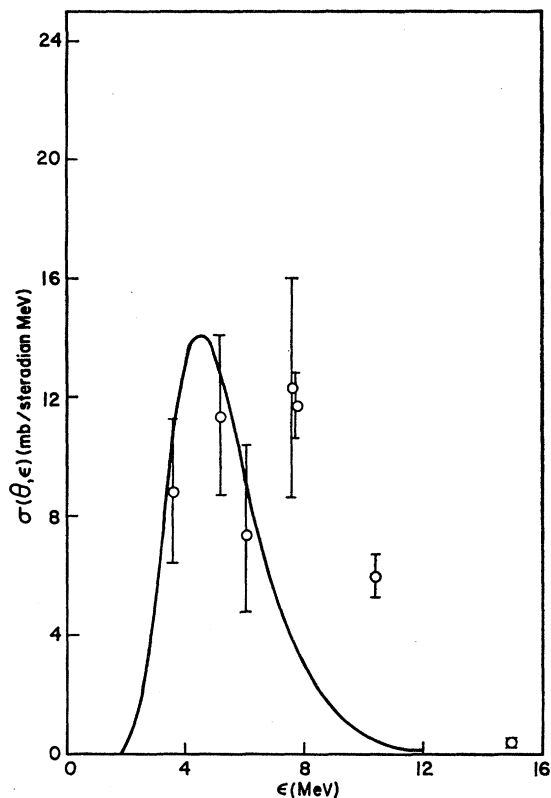


FIG. 4. Proton cross sections at 0° . (The curve represents compound nucleus contribution based on the nuclear temperature of 1.0 MeV).

greatly for higher excitation. A great number of different energy levels in the $\text{Ni}^{(x+n)}$ isotopes will be excited by the relatively broad source of 15-MeV neutrons on Ni^z since the excitation energy is about 22 MeV.

A conventional statistical theory plot is presented of the data at angles of 0° and 138° in Fig. 6. It is seen from this presentation that the cross section is significantly larger for the production of the higher energy protons at 0° than at 138° and that a good fit is obtained to the 138° data with a nuclear temperature of 1.0 MeV. It seems reasonable, therefore, to assume that the data at 138° represents the compound nucleus contribution and the difference between the cross sections at 0° and 138° is attributable to direct interaction processes. Due to the negative Q of the (n, np) reaction, there are no (n, np) protons contributing to data points above 5 MeV. Consequently, the nuclear temperature was determined by fitting the slope to the 138° points above 5 MeV. Note that the (n, np) contribution appears to be very small, surely less than 10%, judging by the fact that the data points at 5.2 MeV and below fit the slope of the nuclear temperature line reasonably well. The $\sigma_c(\epsilon)$'s used were based on the calculations of Shapiro¹⁵ with $r = 1.5A^{1/3} \times 10^{-13}$ cm.

The curves in Figs. 4 and 5 representing contributions to the cross section due to compound nucleus processes

were derived from the nuclear temperature determined in Fig. 6.

The total compound nucleus contribution, as derived from the 138° data assuming an isotropic angular distribution, is 650 ± 150 mb. A total direct interaction contribution is then found to be 160 ± 30 mb making a total cross section of 810 ± 155 mb.

Brown and Muirhead¹⁷ have calculated for 14-MeV neutrons the absolute values of the cross sections of (n, p) reactions resulting from a single collision as well as compound nucleus formation. They predict the total cross section for Ni^{58} as 530 mb and for Ni^{60} as 145 mb. The compound nucleus part is 470 and 115 mb, respectively, thus leaving 60 and 30 mb, respectively, for the direct interaction contribution. Considering natural nickel as 71% Ni^{58} and the remainder Ni^{60} , Brown and Muirhead predict 420 mb as the total cross section with 51 mb of direct interaction contribution. The fraction of direct interaction predicted then becomes $51/420 = 0.12$. The present experiment indicates a total cross section of 810 mb for (n, p) with 160 mb due to direct interaction, leading to a ratio of 0.20. The bombarding energy was about 1 MeV higher than that assumed by Brown and Muirhead which would justify a somewhat

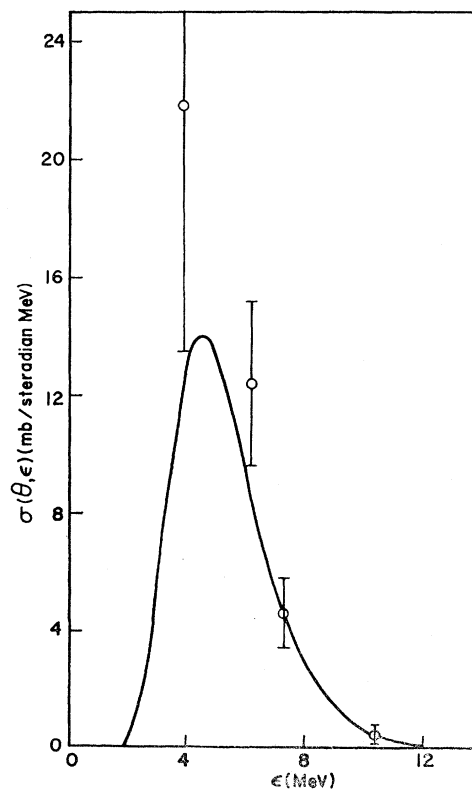


FIG. 5. Proton cross sections at 138° . (The curve represents compound nucleus contribution based on the nuclear temperature of 1.0 MeV.)

¹⁷ G. Brown and H. Muirhead, *Phil. Mag.* **2**, 473 (1957).

TABLE I. Measured and predicted cross sections and nuclear temperatures.

Nucleus	Cross section (mb)				$\sigma(\text{Compound nucleus})$	Nuclear temperature (MeV)	Source
	$\sigma(\text{Total})$	$\sigma(n,p+n,d)$	$\sigma(n,p)$	$\sigma(\text{Direct interaction})$			
Natural Ni			810±170	160±80	650±150	1.0 ±0.1	Present experiment
			255±26	33	222	1.2 ±0.08	Hassler and Peck ^a
Ni ⁵⁸			530	60	470		Brown and Muirhead ^b
Ni ⁵⁸	440±44	282		20		1.0	Kumabe and Fink ^c
Ni ⁵⁸	830±70	515	490	60	430	1.35±0.03	Glover and Purser ^d
Ni ⁵⁸	530±106	310					Allan 1957 ^e
Ni ⁵⁸		440±27				1.1 ±0.1	Allan 1961 ^f
Ni ⁵⁸		534±107				1.58±0.05	Storey, Jack, and Ward ^g
Ni ⁶⁰			145	30	115		Brown and Muirhead ^b
Ni ⁶⁰	300±60	240					Allan 1957 ^e
Ni ⁶⁰		124±9				1.1 ±0.1	Allan 1961 ^f
Ni ⁶⁰		158±32				1.48±0.05	Storey, Jack, and Ward ^g
Ni ⁶⁰	233±25			68	87	1.0	March and Morton ^h

^a See Ref. 8. ^b See Ref. 17. ^c See Ref. 4. ^d See Ref. 6. ^e See Ref. 1. ^f See Ref. 7. ^g See Ref. 5. ^h See Ref. 2.

larger cross section for the present experiment. The ratio of direct interaction to total cross section shows reasonable agreement.

Table I is a summary of the results of the present experiment as well as the results of other investigators studying the charged particles emitted by neutron bombardment of nickel with 14-MeV neutrons. The

third column $\sigma(n,p+n,d)$ represents the cross sections determined by most investigators without separation of the protons from other charged particles. However, recently, Glover and Purser,⁶ as well as Hassler and Peck,⁸ have done experiments with counter telescopes in which protons and deuterons are separately detected. Their results are reported in Table I also.

Our total direct-interaction cross section was determined by normalizing the total direct-interaction contributions of Hassler and Peck, Glover and Purser, and March and Morton,² with the ratio of their direct interaction contribution at 0° to ours at the same angle.

The (n,p) cross sections measured in this experiment as well as those reported by Glover and Purser, and Hassler and Peck, are as large or larger than previous experiments which made no effort to separate the charged particles and thus indicate a small cross section for deuteron emission.

It is apparent that the nuclear temperature determined in the present experiment agrees well with the nuclear temperature found in the experiments measuring both deuterons and protons combined. The direct interaction contribution appears to be comparable to or larger than most previous measurements.

ACKNOWLEDGMENTS

The authors wish to express their sincere appreciation to Professor J. H. Roberts and Professor K. K. Seth of Northwestern University, and to Dr. R. G. Johnson of Lockheed Missiles and Space Company for valuable advice concerning this work, and to Dr. S. Wexler of the Argonne National Laboratory for filling the tritium gas cell.

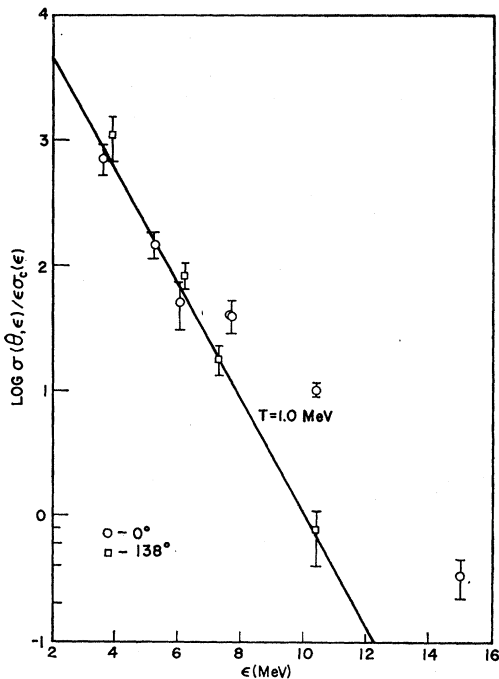


FIG. 6. Conventional statistical theory plot for protons.